Virology 485 (2015) 330–339

Contents lists available at ScienceDirect

Virology

journal homepage: www.elsevier.com/locate/yviro

Severe acute respiratory syndrome coronavirus E protein transports calcium ions and activates the NLRP3 inflammasome

Jose L. Nieto-Torres [a,1], Carmina Verdiá-Báguena [b,1], Jose M. Jimenez-Guardeño [a], Jose A. Regla-Nava [a], Carlos Castaño-Rodriguez [a], Raul Fernandez-Delgado [a], Jaume Torres [c], Vicente M. Aguilella [b,*], Luis Enjuanes [a,*]

[a] Department of Molecular and Cell Biology, National Center of Biotechnology (CNB-CSIC), Campus Universidad Autónoma de Madrid, 28049 Madrid, Spain
[b] Department of Physics, Laboratory of Molecular Biophysics. Universitat Jaume I, 12071 Castellón, Spain
[c] School of Biological Sciences, Division of Structural and Computational Biology, Nanyang Technological University, Singapore 637551, Singapore

ARTICLE INFO

Article history:
Received 29 June 2015
Returned to author for revisions
30 July 2015
Accepted 12 August 2015

Keywords:
SARS-CoV
Coronavirus
E protein
Ion channel
Viroporin
Calcium
Inflammasome
Pathogenesis

ABSTRACT

Severe acute respiratory syndrome coronavirus (SARS-CoV) envelope (E) protein is a viroporin involved in virulence. E protein ion channel (IC) activity is specifically correlated with enhanced pulmonary damage, edema accumulation and death. IL-1β driven proinflammation is associated with those pathological signatures, however its link to IC activity remains unknown. In this report, we demonstrate that SARS-CoV E protein forms protein–lipid channels in ERGIC/Golgi membranes that are permeable to calcium ions, a highly relevant feature never reported before. Calcium ions together with pH modulated E protein pore charge and selectivity. Interestingly, E protein IC activity boosted the activation of the NLRP3 inflammasome, leading to IL-1β overproduction. Calcium transport through the E protein IC was the main trigger of this process. These findings strikingly link SARS-CoV E protein IC induced ionic disturbances at the cell level to immunopathological consequences and disease worsening in the infected organism.

Introduction

Coronaviruses (CoVs) cause respiratory diseases in humans ranging from common colds to fatal pneumonias (Graham et al., 2013; Perlman and Netland, 2009). At the end of 2002, the etiological agent of severe acute respiratory syndrome (SARS-CoV) emerged in Guandong province, Southeast China, initiating a global epidemic. Approximately 8000 people were infected by the virus, whose severe disease resulted in a 10% mortality rate (Drosten et al., 2003; Rota et al., 2003). The SARS-CoV epidemic was controlled by the summer of 2003, and the virus has not naturally reemerged since (http://www.who.int). However, in 2012 a closely related CoV appeared in Saudi Arabia causing the Middle East respiratory syndrome (MERS-CoV) (Zaki et al., 2012). MERS-CoV induces acute pneumonia similar to that caused by SARS-CoV, and is sometimes accompanied with renal failure (Danielsson and Catchpole, 2012; Zaki et al., 2012). MERS-CoV is now circulating and spreading throughout the human population, and to date has infected at least 1356 people leading to death in 484 cases. Initial cases were confined to countries of the Arabian Peninsula; however, new extensive infection clusters have been recently reported in other regions such as South Korea (http://www.who.int). Furthermore, CoVs similar to those causing SARS, MERS, and many other human and animal diseases have been detected in bat species circulating all over the globe (Annan et al., 2013; Chu et al., 2008; Drexler et al., 2010; Falcon et al., 2011; Muller et al., 2007; Quan et al., 2010). Bats are now considered the natural host for most CoVs, providing a perfect scenario for recombination events among different viral species leading to the emergence of new viruses, able to cross species barriers and cause devastating illness in other animals and humans (Graham et al., 2013). For this reason, development and implementation of broad spectrum treatments and general therapeutic strategies against CoVs are a high priority.

CoVs are enveloped viruses containing the largest positive-sense RNA genomes known, around 30 Kb, which encode the viral replicase and a set of structural proteins: spike (S), envelope (E) and membrane (M), present in the viral envelope, and nucleocapsid (N) located inside the viral particle (Enjuanes et al., 2008). The S protein interacts with the cellular receptor to trigger viral entry into the host cell (Enjuanes et al., 2008; Wong et al., 2004). The E and M proteins actively

* Corresponding authors.
E-mail addresses: aguilell@uji.es (V.M. Aguilella), L.Enjuanes@cnb.csic.es (L. Enjuanes).
[1] Both authors equally contributed to this work.

http://dx.doi.org/10.1016/j.virol.2015.08.010
0042-6822/

participate in viral morphogenesis (de Haan et al., 1999; Lim and Liu, 2001; Nguyen and Hogue, 1997; Ruch and Machamer, 2012), and the N protein coats the viral genome to form a helicoidal nucleocapsid that remains protected within the viral envelope (Narayanan et al., 2000). Depending on the CoV species, there are other accessory proteins, some structural, that are also encoded by the genome. SARS-CoV encodes the highest number of accessory genes (3a, 6, 7a 7b, 8a, 8b and 9b), which play diverse roles eventually related to pathogenesis (Enjuanes et al., 2008).

To analyze the mechanisms leading to the high virulence of SARS-CoV and MERS-CoV, several mutants affecting their different genes have been generated (Almazan et al., 2013; DeDiego et al., 2007; DeDiego et al., 2014a; Scobey et al., 2013; Yount et al., 2005). Remarkably, deletion of SARS-CoV E gene produced a virus that was attenuated in at least three different animal models and conferred protection against SARS-CoV challenge (DeDiego et al., 2007, 2008, 2011; Fett et al., 2013; Lamirande et al., 2008; Netland et al., 2010). Small deletions in different domains of the E protein caused similarly attenuated viruses, and are promising vaccine candidates (Regla-Nava et al., 2015). In a similar approach, a MERS-CoV missing the E gene was generated, resulting in a replication-competent, propagation-defective virus which may also constitute the basis of a safe attenuated vaccine (Almazan et al., 2013).

The CoV E gene encodes a small transmembrane protein highly synthesized during infection (Maeda et al., 2001; Nieto-Torres et al., 2011; Raamsman et al., 2000) that mainly localizes to the Golgi apparatus and the endoplasmic reticulum Golgi apparatus intermediate compartment (ERGIC), where it facilitates virus production and morphogenesis (Cohen et al., 2011; Corse and Machamer, 2002; Maeda et al., 2001; Nal et al., 2005; Venkatagopalan et al., 2015). Notably, when the E protein is present, SARS-CoV overstimulates the NF-κB inflammatory pathway (DeDiego et al., 2014b) and, through its PDZ-binding motif, interacts with the cellular protein syntenin, triggering p38 MAPK activation (Jimenez-Guardeño et al., 2014). These signaling cascades result in exacerbated inflammation and immunopathology. The connection between the E protein and virulence has further encouraged the search for other E protein functions that may trigger disease worsening.

One of the most striking functions displayed by the CoV E protein is ion channel (IC) activity. The CoV E protein self assembles in membranes forming pentameric protein-lipid pores that allow ion transport (Pervushin et al., 2009; Torres et al., 2007; Verdia-Baguena et al., 2012; Wilson et al., 2004, 2006). Interestingly, lipid head-groups are integral components of the pore and regulate ion conductance and selectivity (Verdia-Baguena et al., 2012, 2013;). The SARS-CoV E protein showed a mild preference for cations (Na^+, K^+) over anions (Cl^-) when reconstituted in membranes mimicking the charge and composition of those of the ERGIC/Golgi. In this scenario, the E protein IC showed no selectivity for any particular cation (Verdia-Baguena et al., 2012), though the relevance and consequences of these IC properties in a cellular context remains unknown.

Alteration of ion, and specially, Ca^{2+} homeostasis in favor of infection has been already demonstrated in several viral systems. To that end a wide range of viruses encode ion conductive proteins similar to E protein, named viroporins (Nieva et al., 2012). Highly pathogenic RNA viruses such as human immunodeficiency virus-1 (HIV-1), hepatitis C virus (HCV), influenza A virus (IAV), picornaviruses and CoVs, encode one or more of these proteins (Nieva et al., 2012). Viroporins participate in several steps of the life cycle and are usually linked with pathogenesis. Whether IC properties could promote pathways leading to disease worsening has been unknown for a long time. Recently, it was described that point mutations that specifically inhibited SARS-CoV E protein IC activity caused attenuation (Nieto-Torres et al., 2014). Mice infected with E protein IC proficient viruses presented extensive disruption of the pulmonary epithelia and edema accumulation (Nieto-Torres et al., 2014). Edema is the major determinant of acute respiratory distress syndrome (ARDS), the pathology induced by SARS-CoV, leading to death (Graham et al., 2013; Hollenhorst et al., 2011; Matthay and Zemans, 2011). Edema and an IL-1β mediated proinflammatory response was increased in the lung parenchyma when E protein IC activity was present (Nieto-Torres et al., 2014).

IL-1β is a potent proinflammatory cytokine crucial in resolving infectious processes; however, its overproduction has been correlated with diverse severe inflammatory diseases such as asthma, ARDS, gout, atherosclerosis and Parkinson's (Dinarello, 2009; dos Santos et al., 2012; Martinon et al., 2006; Pugin et al., 1996; Strowig et al., 2012). Organisms tightly control IL-1β production through macromolecular complexes called inflammasomes, which are mainly expressed in macrophages and dendritic cells although other cell types, such as those of the bronchiolar epithelium, synthesize their components (Ichinohe et al., 2010; Triantafilou and Triantafilou, 2014). One highly studied inflammasome is the nucleotide-binding oligomerization domain (NOD)-like receptor pyrin domain-containing protein 3 (NLRP3) inflammasome, relevant in the pulmonary tissue. This complex is composed of the sensing protein NLRP3, the adapter component apoptosis-associated speck-like protein containing a caspase activation and recruitment domain (ASC) and the catalytically inactive procaspase-1 (Elliott and Sutterwala, 2015; Latz et al., 2013). The inflammasome components are synthesized under precise danger stimuli, such as molecular patterns associated to infections. However, a second signal is sequentially needed to induce their assembly, which triggers the inflammasome. This leads to the processing of procaspase-1 into active caspase-1, which cleaves inactive pro-IL-1β into its mature form IL-1β that is released to the extracellular media to stimulate proinflammation (Elliott and Sutterwala, 2015; Latz et al., 2013). The presence of ionic imbalances within cells is a main trigger of the NLRP3 inflammasome assembly and activation (Latz et al., 2013). Interestingly, several viroporins stimulate this pathway through alteration of cell ion homeostasis, frequently involving Ca^{2+} imbalances (Ichinohe et al., 2010; Ito et al., 2012; Triantafilou et al., 2013a; Triantafilou and Triantafilou, 2014).

There is clear evidence correlating NLRP3 inflammasomes and IL-1β driven proinflammatory cascades with worsening of several respiratory diseases, including those caused by viruses (dos Santos et al., 2012; McAuley et al., 2013; Pugin et al., 1996; Triantafilou and Triantafilou, 2014). However, the specific role that viral proteins with IC activity may play in this process has not been fully determined. Overproduction of IL-1β in the airways of the lungs of mice infected with E protein IC proficient SARS-CoVs, strongly suggested that ion conductivity may be stimulating the inflammasome (Nieto-Torres et al., 2014). Here we demonstrate that SARS-CoV E protein forms a Ca^{2+} permeable channel in ERGIC/Golgi membranes. E protein IC activity alters Ca^{2+} homeostasis within cells boosting the activation of the NLRP3 inflammasome, which leads to the overproduction of IL-1β. This data supports that SARS-CoV E protein Ca^{2+} channel activity may play a role in disease, through overstimulation of inflammasomes leading to immunopathology. Pharmacological inhibition of this pathway may constitute the basis for combined therapeutics applicable for SARS-CoV and other viruses.

Results

The SARS-CoV E protein forms Ca^{2+} permeable ion channels

Previously, we reported that the SARS-CoV E protein forms channels that are moderately selective for cations in membranes mimicking the ERGIC/Golgi (Verdia-Baguena et al., , 2012, 2013). Within cells, the movement of different cations through the E protein

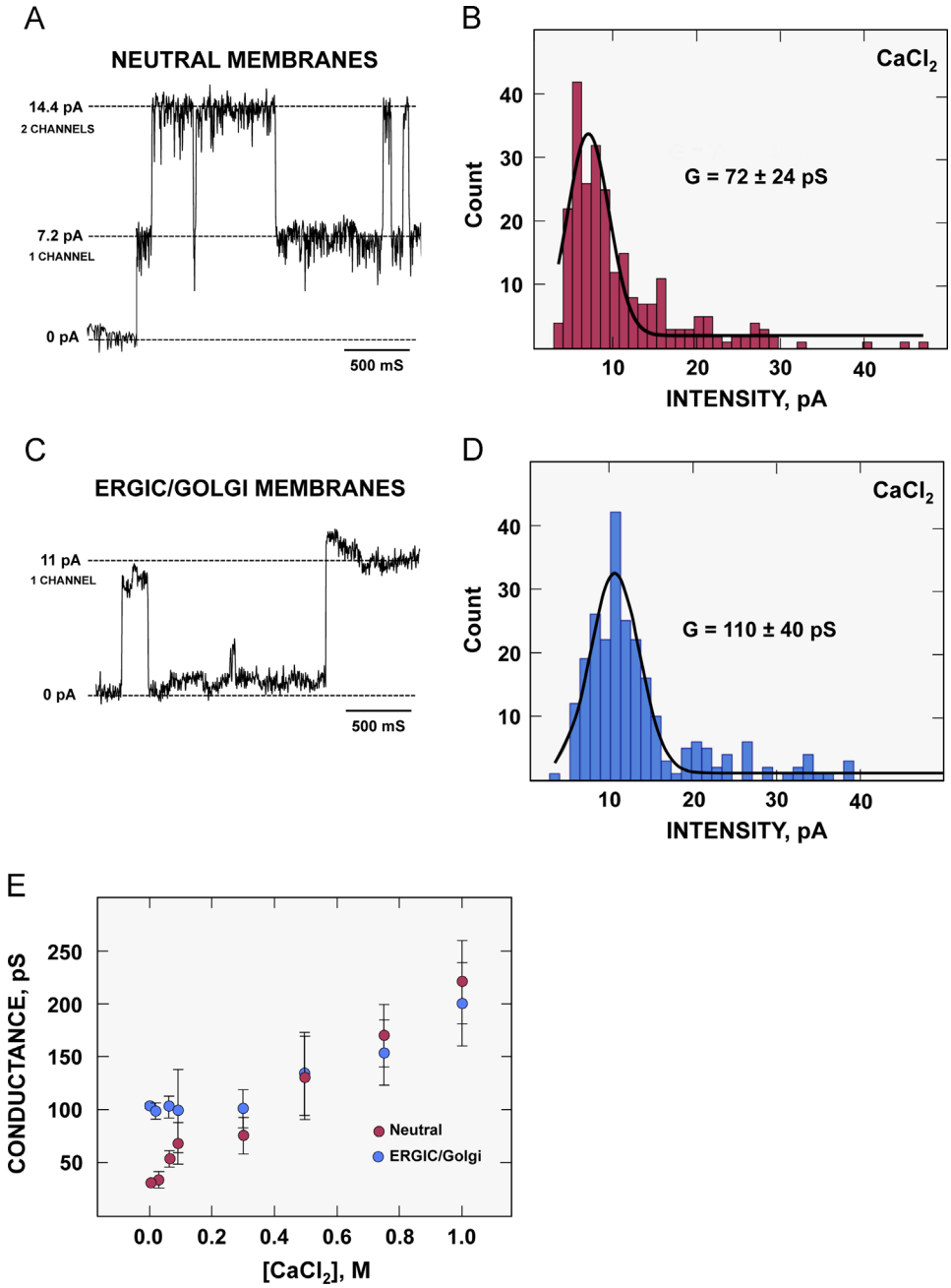

Fig. 1. SARS-CoV E protein IC activity in $CaCl_2$ solutions. (A) Current recordings showing intensity jumps (measured in pA) corresponding to the assembly and disassembly of one or several channels in neutral DPhPC membranes. (B) Histogram representing the intensity of the different current jumps recorded and their respective frequency in neutral membranes. Conductance (G), which is the ratio between current intensity and the applied voltage, is also indicated (measured in pS). Current jumps (C) and their corresponding histogram (D) measured in ERGIC/Golgi membranes. (E) Single-channel conductance variation in solutions containing increasing concentrations of $CaCl_2$. Magenta circles represent data from neutral membranes and blue circles values from ERGIC/Golgi membranes. Error bars show standard deviations from three independent experiments.

pore should be dictated by their respective gradients. Ca^{2+} possesses the highest asymmetrical distribution between the ER-Golgi lumen (hundred μM) and the cytoplasm (around 100 nM) (Zhou et al., 2009), which should allow the flow of this cation through the E protein IC channel if it is permeable. To test whether this is the case, E protein ICs were first reconstituted in artificial neutral lipid membranes in order to exclude any effect coming from the lipid charge, using 100 mM $CaCl_2$ solutions. Current jumps corresponding to the assembly of channels in the lipid membrane were detected (Fig. 1A). The most frequent current jump, representing the insertion of a single E protein IC in the lipid membrane, displayed an intensity of 7.2 ± 2.4 pA. Interestingly, values multiple of 7.2 pA were also detected, corresponding to the insertion of two (14.4 pA) or three channels (21.6 pA), reinforcing the previous observation (Fig. 1A and B). Because lipid charge can affect channel conductance (Verdia-Baguena et al., 2012, 2013), single channel conductance was analyzed in ERGIC/Golgi-like membranes that contained approximately 20% negatively charged lipids. Interestingly, the E protein IC showed a slightly higher unitary current jump of 11 ± 4 pA under these conditions, and multiples of this value, evidencing the insertion of additional channels, were also detected (Figs. 1C and D). The presence of the negatively charged lipid head-groups in the channel pore may facilitate Ca^{2+} flow through the

channel enhancing current intensity under these conditions. This effect was already reported for E protein and monovalent cations (Verdia-Baguena et al., 2012).

Additional measurements were performed in aqueous solutions with decreasing $CaCl_2$ concentrations, to approach Ca^{2+} amounts found in the ERGIC/Golgi lumen. IC conductance (G), which is the ratio between the current intensity and the applied voltage, was calculated. Single channel conductance scaled almost linearly with $CaCl_2$ concentration in neutral membranes (Fig. 1E). This reflects that ion conduction inside the E protein IC is similar to the conduction of the solution, which increases as the electrolyte concentration rises. These data indicate that the interaction between the channel and the permeating ions is weak, and are in accordance with E protein forming a neutral pore in these conditions, as previously reported for monovalent cation salts (Verdia-Baguena et al., 2013). In ERGIC/Golgi membranes two different regimes depending on the range of $CaCl_2$ concentrations were observed. A linear relation between conductance and $CaCl_2$ concentration was again detected in high concentrated solutions. However, IC conductance in ERGIC/Golgi membranes was independent of $CaCl_2$ concentration in low concentration solutions (below 0.2 M), and higher than in neutral membranes (Fig. 1E). This result suggests that E protein acts as a charged protein–lipid pore in ERGIC/Golgi membranes. In this scenario, the conductance is regulated by the balance between the ions that flow into the channel to neutralize the excess of negative charges and the bulk electrolyte concentration. Collectively, these data indicate that the E protein forms channels that are highly conductive in $CaCl_2$. Furthermore, E protein ICs worked very efficiently when reconstituted in ERGIC/Golgi membranes under Ca^{2+} concentrations approaching those found in the lumen of the organelles (hundred μM).

To specifically test E protein selectivity for Ca^{2+}, i.e. the ability of the IC to select Ca^{2+} either by its charge or by its intrinsic properties, reversal potential (Erev) experiments were performed. The rational of these experiments is provided next. ICs were reconstituted in lipid membranes that separated two solutions, one with high and the other with low $CaCl_2$ concentration. This concentration gradient induces the movement of ions through the channel to equilibrate their asymmetric distribution. The potential applied across the channel, which is required to counteract this ion movement leading to zero electric current is the Erev. The Erev can be transformed into channel permeability for Ca^{2+} (PCa^{2+}) and Cl^- (PCl^-) by using the Goldman–Hodgkin–Katz equation (Hodgkin and Katz, 1949). To test whether lipid charge may have an effect on E protein, selectivity measurements were performed in neutral, ERGIC/Golgi similar charged membranes, and fully negative-charged membranes. The E protein IC showed PCa^{2+}/PCl^- values of 0.2 (1/5) in neutral membranes. The value of this permeability ratio is barely the same expected for a non-selective neutral pore just reflecting the different diffusivities of Ca^{2+} and Cl^-. Therefore, E protein channel is equally selective for Cl^- and Ca^{2+} in neutral membranes. Interestingly, the ratio PCa^{2+}/PCl^- increased when the E protein IC was assembled in membranes containing negatively charged lipids, being 0.5 in ERGIC/Golgi membranes and 1.8 in negative membranes (Fig. 2). These data indicated that lipid charge largely influenced the channel preference for Ca^{2+} showing that under conditions mimicking the ERGIC/Golgi environment, E protein displayed a mild selectivity for Ca^{2+}.

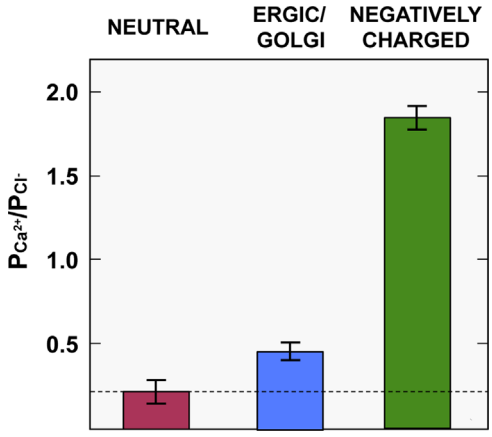

Fig. 2. Ca^{2+} selectivity of SARS-CoV E protein channel. Permeability ratios PCa^{2+}/PCl^- in neutral DPhPC (magenta column), ERGIC/Golgi (blue column) or negatively-charged DPhPS membranes (green column). Dotted line represents the permeability ratio value for a hypothetical neutral pore. Values above the line represent cation selectivity, and those below correspond to anion selectivity. Error bars show standard deviations.

Calcium cations and pH modulate E protein channel selectivity

Multivalent ions, such as Ca^{2+}, can modulate ion transport across ICs by interacting with the internal charges of their pores (Alcaraz et al., 2009; Garcia-Gimenez et al., 2012; Queralt-Martin et al., 2011). Therefore we tested whether E protein ion selectivity could be modified by the presence of a range of small $CaCl_2$ concentrations. Ion selectivity was measured using a ten-fold concentration gradient of KCl at pH 6 upon symmetrical addition of very small $CaCl_2$ concentrations (mM range), at both sides of the membrane. By applying the Erev, the flow of K^+ and Cl^- ions

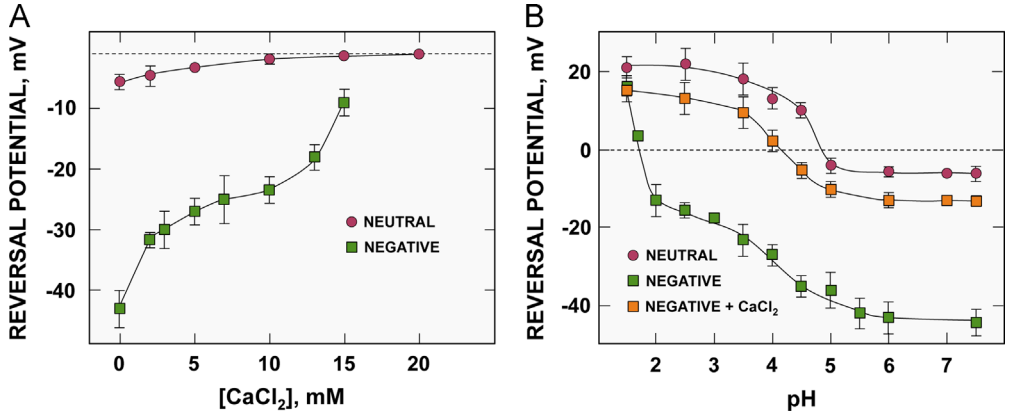

Fig. 3. Modulation of SARS-CoV E protein channel selectivity by Ca^{2+}. (A) Reversal potential (Erev) was measured in asymmetric (500 mM | 50 mM) KCl solutions upon addition of millimolar $CaCl_2$ concentrations. Two series of experiments were performed: in neutral DPhPC (magenta circles) and negatively charged DPhPS membranes (green squares). Dotted line shows Erev value corresponding to a non-selective ion channel. (B) Effect of pH on E protein Erev measured under the same KCl conditions above mentioned in neutral (magenta circles) and negatively charged membranes in the absence (green squares) or the presence of 15 mM $CaCl_2$ (orange squares). Dotted line shows the Erev value corresponding to a non-selective ion channel. Error bars represent standard deviations from three independent experiments.

down their electrochemical potential gradient is prevented. Therefore, Erev measures the relative preference of the channel for K^+ cations over Cl^- anions, but not for Ca^{2+}, because calcium concentrations are the same at both sides of the pore. To analyze the relevance of Ca^{2+} on IC selectivity, this type of experiments were performed in neutral and in negatively-charged membranes (Fig. 3A). In charged membranes the addition of small amounts of Ca^{2+} induced significant changes in the channel Erev, whereas in neutral membranes the effect was very small, although still measurable. These results indicate that Ca^{2+} interaction with E protein channel, modifying the effective pore charge, mainly occur with the lipid charges that line the pore, rather than with acidic residues of E protein TM domain.

Previously we reported that pH also modulates E protein channel selectivity by protonation and deprotonation of the titratable residues present in the pore (Verdia-Baguena et al., 2013). The effect of Ca^{2+} and pH on E protein selectivity was simultaneously tested. Erev titration was studied in the presence or absence of 15 mM $CaCl_2$ under different pH conditions (Fig. 3B). In negatively-charged lipid membranes, rising pH induced sequential deprotonation of lipid head-groups and E protein glutamic acid residues as their respective pK_a (1.73 for lipid head-groups and 4.5 for glutamic acid) were overtaken, conferring an excess of negative charges to the channel and making it cation selective. The addition of Ca^{2+} when E protein is reconstituted in charged membranes reduces the cationic selectivity or increases the anionic selectivity (i.e., it shifts the reversal potential towards less negative values), and reversal potential values become closer to those obtained in neutral membranes. This indicates that Ca^{2+} ions interact with the acidic protein residues and the negative lipid head-groups and decrease the effective negative charge of the E protein pore. This effect was especially patent at physiological values of pH (pH 6–7.5). In addition, this interaction of Ca^{2+} ions with the protein acidic residues shifts their effective pK_a towards lower values. These results indicate that both Ca^{2+} and H^+ ions change E channel transport properties by modifying the charge of the pore, and further support that Ca^{2+} enters within E protein IC.

Identification of SARS-CoV E protein ion channel mutants lacking Ca^{2+} transport

In order to assess the biological impact of SARS-CoV E protein with and without Ca^{2+} channel activity, we evaluated previously constructed mutants containing amino acids substitutions known to affect the E protein IC. Previously we demonstrated that mutations N15A and V25F in the transmembrane domain of SARS-CoV E protein abolished ion conductance in KCl and NaCl solutions (Verdia-Baguena et al., 2012). New conductance measurements were performed in ERGIC/Golgi membranes in 100 mM $CaCl_2$ solutions (Fig. 4). Wildtype E protein transmembrane peptides showed conductance values in the range of 110 pS, whereas no conductance was observed for N15A or V25F mutants, indicating that these mutations also inhibited Ca^{2+} transport, and probably prevent all ion passage as it was previously demonstrated that they also failed to transport K^+, Na^+ and Cl^- (Verdia-Baguena et al., 2012).

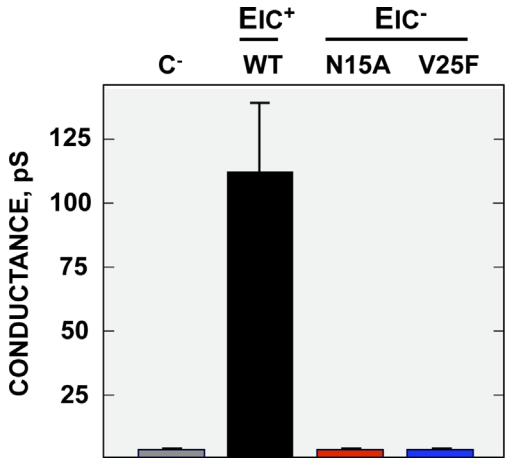

Fig. 4. Mutations inhibiting SARS-CoV E protein conductance in $CaCl_2$. Single channel conductance was measured in 100 mM $CaCl_2$, in the absence of any peptide (C−, gray column), or in the presence of wildtype SARS-CoV E protein transmembrane domain peptide (WT, black column), or the mutant peptides N15A (red column) and V25F (blue column). Error bars represent standard deviations.

Ca^{2+} transport through SARS-CoV E protein channel activates the NLRP3 inflammasome

Alteration of cellular ion homeostasis by SARS-CoV E protein IC could have several implications. Previously, we linked E protein IC with IL-1β triggered proinflammation in the lungs of mice, leading to epithelial cell damage and death (Nieto-Torres et al., 2014). Higher levels of mature IL-1β were detected in the airways of infected animals when E protein IC activity was present, suggesting that ion conductance could stimulate the inflammasome. To determine whether this was the case, the inflammasome complex was reconstituted in Vero E6 cells by transient transfection of its components (NLRP3, ASC and procaspase-1) and the inactive pro-IL-1β (Lo et al., 2013), in the absence or presence of E protein, with or without IC activity. All the components of the inflammasome, besides the different versions of E protein were efficiently expressed within cells (Fig. 5A). When pro-IL-1β was transfected as a control, no significant level of active IL-1β was detected in the supernatant. However, when all the components were supplied to the cells, the inflammasome was stimulated, and active IL-1β was detected in the media in the range of 600 pg/ml (Fig. 5B). Interestingly, the production of IL-1β was significantly enhanced in the presence of E protein with IC activity (IC^+) (> 800 pg/ml). This stimulation was IC activity dependent, as the E protein mutants lacking ion conductance (N15A and V25F), represented in the figure as EIC_1^- and EIC_2^-, respectively, did not boost IL-1β levels (Fig. 5B). Stimulation levels found with wildtype E protein were in the range of those previously reported for other inflammasome activating proteins, using this system (Lo et al., 2013).

Imbalances in Ca^{2+} within cells have been described as an inflammasome inducer (Ito et al., 2012; Murakami et al., 2012; Triantafilou et al., 2013b). To test the specific contribution of SARS-CoV E protein Ca^{2+} transport to inflammasome activation, the complex was reconstituted in cells in the presence or absence of E protein. Cells were subsequently treated with the cell permeant calcium chelator BAPTA-AM (Fig. 6A). This compound enters cells and binds Ca^{2+} preventing inflammasome activation (Ito et al., 2012). Increasing amounts of BAPTA-AM markedly decreased the levels of secreted IL-1β in the presence of E protein (Fig. 6A, INFL EIC^+), reaching levels close to those obtained when the inflammasome was assembled alone (Fig. 6A, INFL). The Ca^{2+} ionophore ionomycin stimulated active IL-1β accumulation in the cell supernatant at levels similar to those seen with E protein, further confirming that Ca^{2+} imbalances boost IL-1β production (Fig. 6B). No significant differences in cell viability were found for any of the treatments (Fig. 6C). Collectively, these results indicate that SARS-CoV E protein activates the NLRP3 inflammasome through its Ca^{2+} transport ability.

Discussion

Ion conductive proteins are widely distributed among viruses, being especially common in RNA viruses (Nieva et al., 2012).

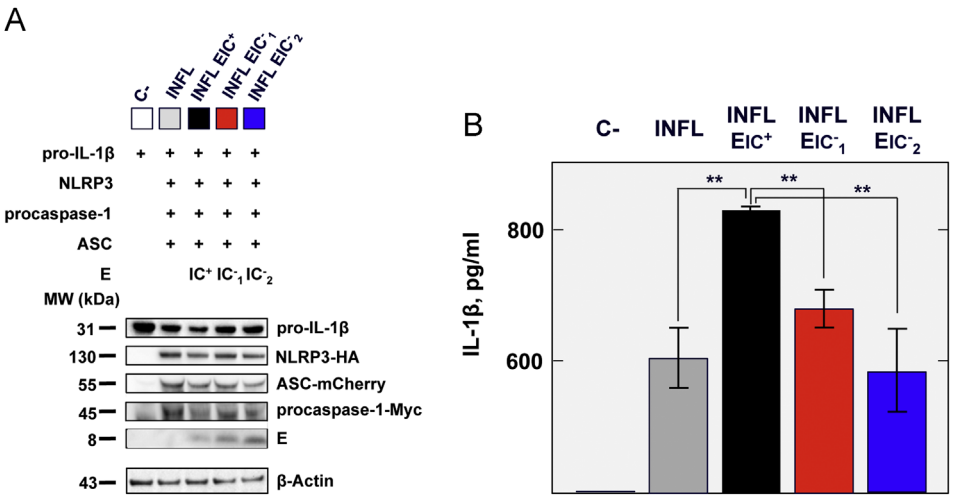

Fig. 5. Inflammasome activation through SARS-CoV E protein ion channel activity. The components of the NLRP3 inflammasome (INFL), NLRP3 (NLRP3-HA), ASC (ASC-mCherry), procaspase-1 (procaspase-1-Myc) and pro-IL-1β were transfected in Vero E6 cells, in the absence or presence of SARS-CoV E protein with (IC^+) or without (IC^-) ion channel activity. EIC_1^- represents the N15A mutant and EIC_2^- indicates the V25F mutant. As a negative control, cells were transfected solely with pro-IL-1β (C−). (A) Western blot showing the presence of the inflammasome complex components and E protein within Vero E6 cells lysates. β-Actin was also detected as a loading control. (B) Levels of active IL-1β present in the cell supernatant. Error bars represent standard deviations from three independent experiments. Statistically significant data are indicated with two asterisks (Student's *t*-test *p* value < 0.01).

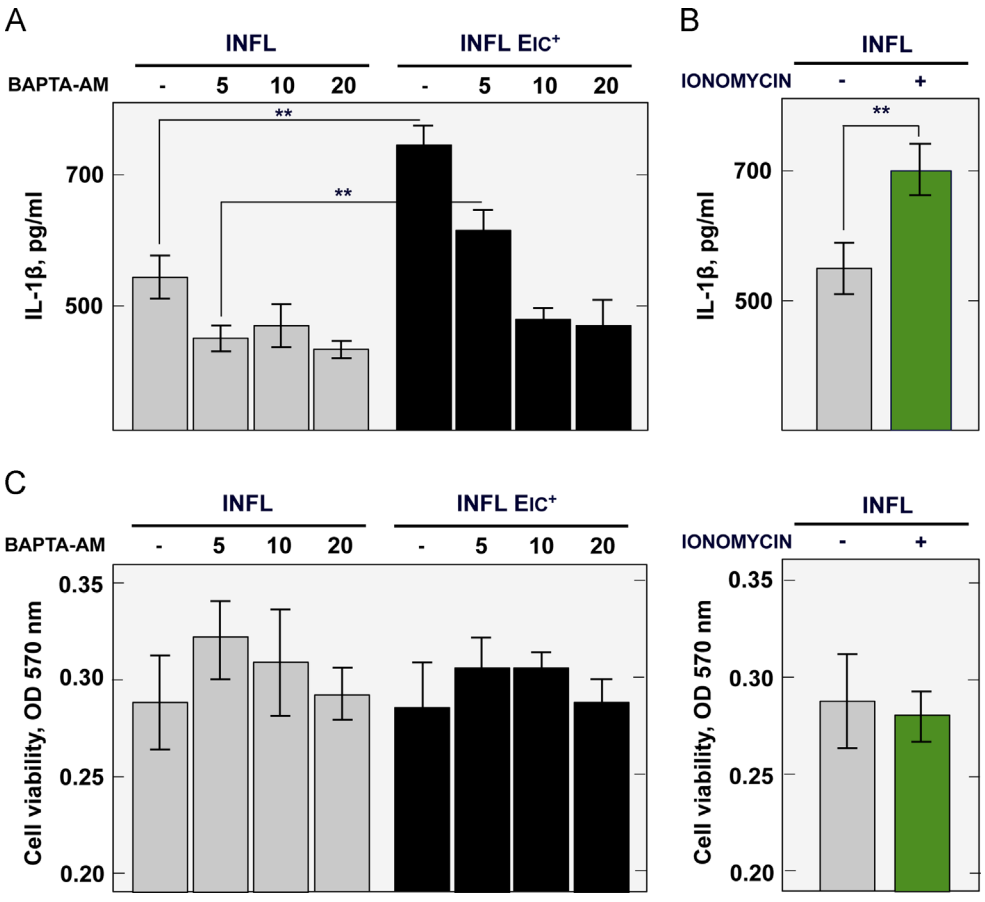

Fig. 6. Inflammasome activation through SARS-CoV E protein Ca^{2+} channel activity. (A) The inflammasome complex (INFL) was reconstituted in cells without or with wildtype E protein (EIC^+) in the presence of increasing concentrations (μM) of the cell permeable Ca^{2+} chelator BAPTA-AM. DMSO was added as negative control (−). The levels of active IL-1β present in the cell media were measured by ELISA. (B) Activation of the inflammasome by the Ca^{2+} ionophore ionomycin. Error bars represent standard deviations from three independent experiments; statistically significant data are indicated with two asterisks (Student's *t*-test *p* value < 0.01). (C) Cell viability MTT assay. Optical densities (OD) representing cellular metabolic activity under the different experimental conditions were measured at 570 nm.

Conductance of ions facilitate diverse processes of the viral life cycle such as entry, takeover of organelles to serve as platforms for viral replication, protection of viral proteins from acidic cell compartments, and trafficking of nascent virions (Nieva et al., 2012). In addition, viroporins are often linked to pathogenesis, and in general, mutant viruses lacking them are attenuated, in many cases serving as effective

vaccines (DeDiego et al., 2007; Netland et al., 2010; Watanabe et al., 2009; Whitehead et al., 1999). Viroporin removal is frequently accompanied by a defect in viral production, which by itself can explain virulence attenuation. However, recent studies have indicated that IC activity may specifically trigger pathways leading to pathology. Previously we demonstrated that SARS-CoVs proficient in E protein IC activity caused increased damage of the pulmonary epithelia and edema accumulation (Nieto-Torres et al., 2014). These disease symptoms correlated with an immunopathological response mediated by proinflammatory cytokines such as IL-6, TNF and IL-1β, the latter being a crucial mediator of this cascade. IL-1β overproduction is linked to a wide range of inflammatory pathologies including those caused by respiratory viruses (dos Santos et al., 2012; McAuley et al., 2013; Pugin et al., 1996; Triantafilou and Triantafilou, 2014). Here, we report for the first time that CoV E protein formed an IC that transported Ca^{2+} in ERGIC/Golgi membranes, where this protein locates, which may have important consequences on cell physiology. In fact, Ca^{2+} leakage through E protein IC induced the activation of the NLRP3 inflammasome resulting in overproduction of IL-1β. This finding together with previous *in vivo* observations indicates that IC activity correlates with proinflammation and pathology.

Generally, viroporins form poorly selective ion channels (Nieva et al., 2012). Therefore, the subcellular location where viroporins assemble and the conditions of that particular environment are crucial determinants of their impact on cellular ionic homeostasis. Previously, we reported that SARS-CoV E protein showed mild selectivity for cations (Na^+ and K^+) when reconstituted in ERGIC/Golgi membranes, mostly conferred by the negative charges of the lipids (Verdia-Baguena et al., 2012, 2013). High concentration gradients are found for Na^+ and K^+ between the cell interior and the extracellular media (Dubyak, 2004). However, there is no known asymmetric distribution for either of these ion species between the lumen of ERGIC/Golgi and the cell cytoplasm (Chandra et al., 1991; Schapiro and Grinstein, 2000). Accordingly, minimal net transport of Na^+ and K^+ through E protein pore should be expected, and therefore the biological relevance of these processes may be also limited. In contrast, the ER and Golgi apparatus store high amounts of calcium ions by the action of pumps such as the sarcoendoplasmic reticulum Ca^{2+} ATPase (SERCA) and the secretory pathway Ca^{2+} ATPase (SPCA) (Wuytack et al., 2002). This creates an enormous gradient of around 1000-fold between the lumen of these organelles and the cytoplasm (Zhou et al., 2009). The gradient allows controlled eventual and temporal leakages of Ca^{2+} into the cytoplasm that trigger several processes relevant to cell physiology. Interestingly, we have shown above that SARS-CoV E protein IC was also permeable to Ca^{2+} in ERGIC/Golgi membranes. Furthermore, Ca^{2+} interacted with the negative charges of the protein-lipid pore, modulating its properties. Several other viroporins are known to transport Ca^{2+}, resulting in leakage of this cation from its intracellular stores. Rotavirus NSP4 protein as well as Coxsackievirus, encephalomyocarditis virus, and poliovirus 2B proteins deplete ER and/or Golgi Ca^{2+} concentrations in favor of viral proliferation (Campanella et al., 2004; Crawford et al., 2012; de Jong et al., 2008). Alteration of protein trafficking, manipulation of apoptosis, and control of autophagy are some of the processes controlled by these Ca^{2+} effluxes. Whether some of these aspects are influenced in a similar manner during SARS-CoV infection will be explored in future experiments.

Protons (H^+) are also actively confined to the lumen of the Golgi apparatus and those of the organelles of the secretory pathway in a process that acidifies their interior and creates a gradient with the cytoplasm (Paroutis et al., 2004). Considering that the E protein IC weakly interacts with circulating ions and that pH can modulate its net charge, it is highly likely that protons will also flow through the IC within cells. This is not an isolated case, as several viroporins such as HCV p7 and IAV M2 are known to transport protons, and others such as the 2B protein of the *picornaviridae* family transport both H^+ and Ca^{2+} (de Jong et al., 2006; Wang et al., 1994; Wozniak et al., 2010). Alkalinization of the Golgi lumen is crucial to protect acid-sensitive viral progeny and prevent premature activation of viral proteins involved in entry processes (Sakaguchi et al., 1996; Wozniak et al., 2010). SARS-CoV E protein IC mutants did not show profound growth defects, although they were outgrown in competition assays by IC proficient viruses, which suggests better proliferation when E protein ion conductance was present (Nieto-Torres et al., 2014). Whether alkalization of intracellular compartments by E protein IC may assist in SARS-CoV production remains to be explored. Besides these considerations, it cannot be excluded that IC activity may have a greater impact in SARS-CoV production. Inhibition of E protein IC activity may be compensated by the action of two other viroporins encoded by SARS-CoV, the 3a and 8a (Chen et al., 2011; Lu et al., 2006); further experiments are being performed to answer this question.

Disruption of ion homeostasis can have profound deleterious effects for the cells; consequently, they have evolved mechanisms to sense and control these disturbances. Ion imbalances associated with infecting pathogens are recognized by inflammasomes, which are components of the innate immune system. Inflammasomes orchestrate proinflammatory responses to fight viral infections, IL-1β being one of the major players (Strowig et al., 2012). However, increasing evidence indicates that overstimulation of this pathway can lead to undesirable effects for the organism. In fact, immunopathology rather than direct viral destruction of infected cells is the main cause of severe disease in many viral illnesses (McAuley et al., 2013; Meduri et al., 1995; Triantafilou and Triantafilou, 2014). SARS-CoVs that lack E protein IC activity induced less proinflammation and active IL-1β, suggesting that IC activity could be a trigger of this pathway (Nieto-Torres et al., 2014). Indeed, wildtype E protein but not its IC^- mutants boosted the production of mature IL-1β through the mediation of a reconstituted inflammasome. Ca^{2+} was the main trigger of this process, as chelation of this ion abolished enhanced IL-1β production, and a Ca^{2+} ionophore produced a similar simulation. E proteins from other human respiratory CoVs, such as MERS-CoV and HCoV-229E, also display ion channel properties (Surya et al., 2015; Verdia-Baguena et al., 2012; Wilson et al., 2006). Investigating whether these proteins may favor Ca^{2+} transport and activation of the inflammasome represents a relevant issue. Furthermore, the identification of a possible correlation between the extent of inflammasome activation and the disease symptoms caused by these viruses, highly deleterious in the case of SARS-CoV and MERS-CoV, and mild in the case of HCoV-229E, could provide key information on the impact of this pathway on the pathological outcome induced by different CoVs, and will be analyzed in future experiments.

This study provides new insights into the molecular mechanisms governing CoV viroporin activity and the consequences of this function in viral pathogenesis. What is more, IL-1β overproduction has been related with the pathology induced by SARS-CoV and other respiratory viruses (Triantafilou and Triantafilou, 2014). Our results suggest that development of specific IC inhibitors and implementation of novel compounds decreasing inflammasome driven immunopathology (Coll et al., 2015) may be a valuable complement to other antiviral approaches for the treatment of these infectious diseases.

Materials and methods

Cells

The African green monkey kidney-derived Vero E6 cells were kindly provided by Eric Snijder (Medical Center, University of Leiden, The Netherlands). Cells were grown at 37 °C with an

atmosphere of 98% humidity and 5% CO_2, in Dulbecco's modified Eagle medium (DMEM, GIBCO) supplemented with 25 mM HEPES, 2 mM L-glutamine (SIGMA), 1% non-essential amino acids (SIGMA) and 10% fetal bovine serum (FBS, BioWhittaker).

Peptide synthesis and ion channel measurements in artificial lipid membranes

Synthetic peptides representing the full-length SARS-CoV E protein, or its transmembrane domain (amino acids 7–38) containing point mutations that inhibited ion channel activity (N15A and V25F), were generated by standard phase synthesis and purified by HPLC, as previously described (Verdia-Baguena et al., 2012). Ion channels were reconstituted in lipid membranes composed of diphytanoyl phosphatidylcholine (DPhPC), diphytanoyl phosphatidylserine (DPhPS), or a mixture of 59% dioleoyl phosphatidylcholine (DOPC), 24% dioleoyl phosphatidylethanolamine (DOPE), and 17% dioleoyl phosphatidylserine (DOPS) (Avanti polar lipids, Inc., Alabaster, AL). The membranes separated two chambers filled with electrolytic solutions of $CaCl_2$ or KCl. Ion channel insertion was achieved by adding 0.5–1 µl of a 300 µg/ml solution of synthetic protein or peptides in a acetonitrile:isopropanol (40:60) buffer to one of the chambers (cis). All measurements were performed at room temperature (23 ± 1 °C).

The single-channel conductance was obtained from current measurements under an applied potential of $^{+}100$ mV in symmetrical salt solutions of 1 M $CaCl_2$ buffered with 5 mM HEPES at pH 6. The conductance values were evaluated using the Gaussian fit tool of Sigma Plot 10.0 (Systat Software, Inc).

For the selectivity measurements the reversal potential (Erev) was obtained under a ten-fold salt concentration gradient (500 mM / 50 mM). One or several channels were inserted into the bilayer causing a net ionic current due to the concentration gradient. Then the ionic current was manually set to zero by adjusting the applied potential. The potential needed to achieve zero current represents the Erev; conversion of Erev into the channel permeability (P_+/P_-) was by done using the Goldman–Hodgkin–Katz (GHK) equation (Hodgkin and Katz, 1949). The effect of Ca^{2+} on E protein ion selectivity was defined by measuring Erev in a ten-fold KCl concentration gradient (500 mM/50 mM) buffered with 5 mM HEPES at pH 6, in the presence of increasing concentrations of $CaCl_2$. The functional interaction of Ca^{2+} with E protein–lipid pore was evaluated measuring Erev in DPhPC and DPhPS membranes under different pH values, with or without 15 mM $CaCl_2$.

Inflammasome reconstitution in Vero E6 cells

Sub-confluent monolayers of Vero E6 cells seeded onto 24-well plates were transfected using Lipofectamine 2000 (Invitrogen) and a set of plasmids encoding the components of the NLRP3 inflammasome (Lo et al., 2013; Wu et al., 2014): 200 ng of pcDNA4-proIL-1β, 25 ng of pcDNA4-NLRP3-HA, 20 ng pcDNA4-ASC-mCherry, and 10 ng of pcDNA4-procaspase-1-Myc, with 100 ng of empty pcDNA3, as a control, or 100 ng of either pcDNA3-E, pcDNA3-EN15A or pcDNA3-EV25F. Cell lysates and culture supernatants were collected 24 h after transfection. The secreted active IL-1β was measured by ELISA according to the manufacturer's specifications (eBioscience).

Cell protein extract preparation and western blot assays

Cells were lysed in a buffer containing Tris/HCl 10 mM, EDTA 1 mM, NaCl 150 mM, IGEPAL 1%, and complete protease inhibitor (Roche) at pH 8. Inflammasome proteins were detected by western blot using a mouse anti-HA antibody (Sigma) to detect NRLP3-HA, mouse anti-mCherry (Abcam) to bind ASC-mCherry, rabbit anti-Myc (Abcam) to label procaspase-1-Myc, and rabbit anti-human IL-1β (Cell signaling). SARS-CoV E protein was detected using a polyclonal antiserum produced in rabbits (Nieto-Torres et al., 2011). As a loading control, beta-actin was labeled using a mouse monoclonal antibody (Abcam). Bound antibodies were detected using HRP-conjugated goat anti-rabbit IgG and rabbit anti-mouse IgG and the Immobilon Western chemiluminicesce substrate (Millipore), following manufacturer's specifications.

Effect of BAPTA-AM and ionomycin treatments on inflammasome activation

Fresh supplemented DMEM containing the indicated concentration of the cell permeant calcium chelator BAPTA-AM (Life technologies) was added to cells 4 h after transfection of the inflammasome components and incubated 30 min at 37 °C. Then, media was removed and a second treatment with fresh media containing BAPTA-AM was performed. Supernatants were collected 20 h post-BAPTA-AM treatment. Ionomycin (Life technologies) was added at 1 µM 4 h after transfection and incubated for 20 h.

Cell viability assay

The MTT colorimetric method was used to measure cell metabolic activity. Cell media of transfected cells was replaced by fresh DMEM supplemented with 10% FCS and 500 µg/ml of MTT. Cells were incubated 2 h at 37 °C. After that, media was removed and a solution containing 0.04 M HCl 0.1% Nonidet P-40 in isopropanol was added. Plates were gently mixed to obtain a homogeneous solution, and optic density was measured at 570 nm.

Acknowledgments

The work done by the authors was supported by Grants from the Government of Spain (BIO2013-42869-R, FIS2013-40473-P), Generalitat Valenciana (Prometeo 2012/069), Fundació Caixa Castelló-Bancaixa (P1-1B2012-03) and a U.S. National Institutes of Health (NIH) project (5P01 AI060699). JLN, JMJ and JAR received contracts from NIH. CCR received a contract from Fundacion La Caixa. We thank professor Ming-Zong Lai (Institute of Molecular Biology, Taipei) for kindly providing us plasmids encoding the inflammasome components. We thank Marga Gonzalez for her technical assistance.

References

Alcaraz, A., Nestorovich, E.M., Lopez, M.L., Garcia-Gimenez, E., Bezrukov, S.M., Aguilella, V.M., 2009. Diffusion, exclusion, and specific binding in a large channel: a study of OmpF selectivity inversion. Biophys. J. 96, 56–66.

Almazan, F., DeDiego, M.L., Sola, I., Zuñiga, S., Nieto-Torres, J.L., Marquez-Jurado, S., Andres, G., Enjuanes, L., 2013. Engineering a replication-competent, propagation-defective Middle East respiratory syndrome coronavirus as a vaccine candidate. mBio 4, e00650–00613.

Annan, A., Baldwin, H.J., Corman, V.M., Klose, S.M., Owusu, M., Nkrumah, E.E., Badu, E.K., Anti, P., Agbenyega, O., Meyer, B., Oppong, S., Sarkodie, Y.A., Kalko, E.K., Lina, P.H., Godlevska, E.V., Reusken, C., Seebens, A., Gloza-Rausch, F., Vallo, P., Tschapka, M., Drosten, C., Drexler, J.F., 2013. Human betacoronavirus 2c EMC/2012-related viruses in Bats, Ghana and Europe. Emerg. Infect. Dis. 19, 456–459.

Campanella, M., de Jong, A.S., Lanke, K.W., Melchers, W.J., Willems, P.H., Pinton, P., Rizzuto, R., van Kuppeveld, F.J., 2004. The coxsackievirus 2B protein suppresses apoptotic host cell responses by manipulating intracellular Ca^{2+} homeostasis. J. Biol. Chem. 279, 18440–18450.

Chandra, S., Kable, E.P., Morrison, G.H., Webb, W.W., 1991. Calcium sequestration in the Golgi apparatus of cultured mammalian cells revealed by laser scanning confocal microscopy and ion microscopy. J. Cell Sci. 100, 747–752.

Chen, C.C., Kruger, J., Sramala, I., Hsu, H.J., Henklein, P., Chen, Y.M., Fischer, W.B., 2011. ORF8a of SARS-CoV forms an ion channel: experiments and molecular dynamics simulations. Biochim. Biophys. Acta 1808, 572–579.

Chu, D.K., Peiris, J.S., Chen, H., Guan, Y., Poon, L.L., 2008. Genomic characterizations of bat coronaviruses (1A, 1B and HKU8) and evidence for co-infections in Miniopterus bats. J. Gen. Virol. 89, 1282–1287.
Cohen, J.R., Lin, L.D., Machamer, C.E., 2011. Identification of a Golgi complex-targeting signal in the cytoplasmic tail of the severe acute respiratory syndrome coronavirus envelope protein. J. Virol. 85, 5794–5803.
Coll, R.C., Robertson, A.A., Chae, J.J., Higgins, S.C., Munoz-Planillo, R., Inserra, M.C., Vetter, I., Dungan, L.S., Monks, B.G., Stutz, A., Croker, D.E., Butler, M.S., Haneklaus, M., Sutton, C.E., Nunez, G., Latz, E., Kastner, D.L., Mills, K.H., Masters, S.L., Schroder, K., Cooper, M.A., O'Neill, L.A., 2015. A small-molecule inhibitor of the NLRP3 inflammasome for the treatment of inflammatory diseases. Nat. Med. 21, 248–255.
Corse, E., Machamer, C.E., 2002. The cytoplasmic tail of infectious bronchitis virus E protein directs Golgi targeting. J. Virol. 76, 1273–1284.
Crawford, S.E., Hyser, J.M., Utama, B., Estes, M.K., 2012. Autophagy hijacked through viroporin-activated calcium/calmodulin-dependent kinase kinase-beta signaling is required for rotavirus replication. Proc. Natl. Acad. Sci. USA 109, E3405–E3413.
Danielsson, N., Catchpole, M., 2012. Novel coronavirus associated with severe respiratory disease: case definition and public health measures. Euro Surveill. 17, 20282.
de Haan, C.A.M., Smeets, M., Vernooij, F., Vennema, H., Pottier, P.J.M., 1999. Mapping of the coronavirus membrane protein domains involved in interaction with the spike protein. J. Virol. 73, 7441–7452.
de Jong, A.S., de Mattia, F., Van Dommelen, M.M., Lanke, K., Melchers, W.J., Willems, P.H., van Kuppeveld, F.J., 2008. Functional analysis of picornavirus 2B proteins: effects on calcium homeostasis and intracellular protein trafficking. J. Virol. 82, 3782–3790.
de Jong, A.S., Visch, H.J., de Mattia, F., van Dommelen, M.M., Swarts, H.G., Luyten, T., Callewaert, G., Melchers, W.J., Willems, P.H., van Kuppeveld, F.J., 2006. The coxsackievirus 2B protein increases efflux of ions from the endoplasmic reticulum and Golgi, thereby inhibiting protein trafficking through the Golgi. J. Biol. Chem. 281, 14144–14150.
DeDiego, M.L., Alvarez, E., Almazan, F., Rejas, M.T., Lamirande, E., Roberts, A., Shieh, W.J., Zaki, S.R., Subbarao, K., Enjuanes, L., 2007. A severe acute respiratory syndrome coronavirus that lacks the E gene is attenuated in vitro and in vivo. J. Virol. 81, 1701–1713.
DeDiego, M.L., Nieto-Torres, J.L., Jimenez-Guardeño, J.M., Regla-Nava, J.A., Alvarez, E., Oliveros, J.C., Zhao, J., Fett, C., Perlman, S., Enjuanes, L., 2011. Severe acute respiratory syndrome coronavirus envelope protein regulates cell stress response and apoptosis. PLoS Pathog. 7, e1002315.
DeDiego, M.L., Nieto-Torres, J.L., Jimenez-Guardeño, J.M., Regla-Nava, J.A., Castaño-Rodriguez, C., Fernandez-Delgado, R., Usera, F., Enjuanes, L., 2014a. Coronavirus virulence genes with main focus on SARS-CoV envelope gene. Virus Res. 194, 124–137.
DeDiego, M.L., Nieto-Torres, J.L., Regla-Nava, J.A., Jimenez-Guardeño, J.M., Fernandez-Delgado, R., Fett, C., Castaño-Rodriguez, C., Perlman, S., Enjuanes, L., 2014b. Inhibition of NF-kappaB mediated inflammation in severe acute respiratory syndome coronavirus-infected mice increases survival. J. Virol. 88, 913–924.
DeDiego, M.L., Pewe, L., Alvarez, E., Rejas, M.T., Perlman, S., Enjuanes, L., 2008. Pathogenicity of severe acute respiratory coronavirus deletion mutants in hACE-2 transgenic mice. Virology 376, 379–389.
Dinarello, C.A., 2009. Interleukin-1beta and the autoinflammatory diseases. N. Engl. J. Med. 360, 2467–2470.
dos Santos, G., Kutuzov, M.A., Ridge, K.M., 2012. The inflammasome in lung diseases. Am. J. Physiol. Lung Cell. Mol. Physiol. 303, L627–L633.
Drexler, J.F., Gloza-Rausch, F., Glende, J., Corman, V.M., Muth, D., Goettsche, M., Seebens, A., Niedrig, M., Pfefferle, S., Yordanov, S., Zhelyazkov, L., Hermanns, U., Vallo, P., Lukashev, A., Muller, M.A., Deng, H., Herrler, G., Drosten, C., 2010. Genomic characterization of severe acute respiratory syndrome-related coronavirus in European bats and classification of coronaviruses based on partial RNA-dependent RNA polymerase gene sequences. J. Virol. 84, 11336–11349.
Drosten, C., Gunther, S., Preiser, W., van der Werf, S., Brodt, H.R., Becker, S., Rabenau, H., Panning, M., Kolesnikova, L., Fouchier, R.A., Berger, A., Burguiere, A.M., Cinatl, J., Eickmann, M., Escriou, N., Grywna, K., Kramme, S., Manuguerra, J.C., Muller, S., Rickerts, V., Sturmer, M., Vieth, S., Klenk, H.D., Osterhaus, A.D., Schmitz, H., Doerr, H.W., 2003. Identification of a novel coronavirus in patients with severe acute respiratory syndrome. N. Engl. J. Med. 348, 1967–1976.
Dubyak, G.R., 2004. Ion homeostasis, channels, and transporters: an update on cellular mechanisms. Adv. Physiol. Educ. 28, 143–154.
Elliott, E.I., Sutterwala, F.S., 2015. Initiation and perpetuation of NLRP3 inflammasome activation and assembly. Immunol. Rev. 265, 35–52.
Enjuanes, L., Gorbalenya, A.E., de Groot, R.J., Cowley, J.A., Ziebuhr, J., Snijder, E.J., 2008. The Nidovirales. In: Mahy, B.W.J., Van Regenmortel, M., Walker, P., Majumder-Russell, D. (Eds.), Third ed. Elsevier Ltd., Oxford, pp. 419–430.
Falcon, A., Vazquez-Moron, S., Casas, I., Aznar, C., Ruiz, G., Pozo, F., Perez-Brena, P., Juste, J., Ibanez, C., Garin, I., Aihartza, J., Echevarria, J.E., 2011. Detection of alpha and betacoronaviruses in multiple Iberian bat species. Arch. Virol. 156, 1883–1890.
Fett, C., DeDiego, M.L., Regla-Nava, J.A., Enjuanes, L., Perlman, S., 2013. Complete protection against severe acute respiratory syndrome coronavirus-mediated lethal respiratory disease in aged mice by immunization with a mouse-adapted virus lacking E protein. J. Virol. 87, 6551–6559.
Garcia-Gimenez, E., Alcaraz, A., Aguilella, V.M., 2012. Divalent metal ion transport across large biological ion channels and their effect on conductance and selectivity. Biochem. Res. Int. 2012, 245786.
Graham, R.L., Donaldson, E.F., Baric, R.S., 2013. A decade after SARS: strategies for controlling emerging coronaviruses. Nat. Rev. Microbiol. 11, 836–848.
Hodgkin, A.L., Katz, B., 1949. The effect of sodium ions on the electrical activity of giant axon of the squid. J. Physiol. 108, 37–77.
Hollenhorst, M.I., Richter, K., Fronius, M., 2011. Ion transport by pulmonary epithelia. J. Biomed. Biotechnol. 2011, 174306.
Ichinohe, T., Pang, I.K., Iwasaki, A., 2010. Influenza virus activates inflammasomes via its intracellular M2 ion channel. Nat. Immunol. 11, 404–410.
Ito, M., Yanagi, Y., Ichinohe, T., 2012. Encephalomyocarditis virus viroporin 2B activates NLRP3 inflammasome. PLoS Pathog. 8, e1002857.
Jimenez-Guardeño, J.M., Nieto-Torres, J.L., DeDiego, M.L., Regla-Nava, J.A., Fernandez-Delgado, R., Castaño-Rodriguez, C., Enjuanes, L., 2014. The PDZ-binding motif of severe acute respiratory syndrome coronavirus envelope protein Is a determinant of viral pathogenesis. PLoS Pathog. 10, e1004320.
Lamirande, E.W., DeDiego, M.L., Roberts, A., Jackson, J.P., Alvarez, E., Sheahan, T., Shieh, W.J., Zaki, S.R., Baric, R., Enjuanes, L., Subbarao, K., 2008. A live attenuated SARS coronavirus is immunogenic and efficacious in golden Syrian hamsters. J. Virol. 82, 7721–7724.
Latz, E., Xiao, T.S., Stutz, A., 2013. Activation and regulation of the inflammasomes. Nat. Rev. Immunol. 13, 397–411.
Lim, K.P., Liu, D.X., 2001. The missing link in coronavirus assembly. Retention of the avian coronavirus infectious bronchitis virus envelope protein in the pre-Golgi compartments and physical interaction between the envelope and membrane proteins. J. Biol. Chem. 276, 17515–17523.
Lo, Y.H., Huang, Y.W., Wu, Y.H., Tsai, C.S., Lin, Y.C., Mo, S.T., Kuo, W.C., Chuang, Y.T., Jiang, S.T., Shih, H.M., Lai, M.Z., 2013. Selective inhibition of the NLRP3 inflammasome by targeting to promyelocytic leukemia protein in mouse and human. Blood 121, 3185–3194.
Lu, W., Zheng, B.J., Xu, K., Schwarz, W., Du, L., Wong, C.K., Chen, J., Duan, S., Deubel, V., Sun, B., 2006. Severe acute respiratory syndrome-associated coronavirus 3a protein forms an ion channel and modulates virus release. Proc. Natl. Acad. Sci. USA 103, 12540–12545.
Maeda, J., Repass, J.F., Maeda, A., Makino, S., 2001. Membrane topology of coronavirus E protein. Virology 281, 163–169.
Martinon, F., Petrilli, V., Mayor, A., Tardivel, A., Tschopp, J., 2006. Gout-associated uric acid crystals activate the NALP3 inflammasome. Nature 440, 237–241.
Matthay, M.A., Zemans, R.L., 2011. The acute respiratory distress syndrome: pathogenesis and treatment. Annu. Rev. Pathol. 6, 147–163.
McAuley, J.L., Tate, M.D., MacKenzie-Kludas, C.J., Pinar, A., Zeng, W., Stutz, A., Latz, E., Brown, L.E., Mansell, A., 2013. Activation of the NLRP3 inflammasome by IAV virulence protein PB1-F2 contributes to severe pathophysiology and disease. PLoS Pathog. 9, e1003392.
Meduri, G.U., Headley, S., Kohler, G., Stentz, F., Tolley, E., Umberger, R., Leeper, K., 1995. Persistent elevation of inflammatory cytokines predicts a poor outcome in ARDS. Plasma IL-1 beta and IL-6 levels are consistent and efficient predictors of outcome over time. Chest 107, 1062–1073.
Muller, M.A., Paweska, J.T., Leman, P.A., Drosten, C., Grywna, K., Kemp, A., Braack, L., Sonnenberg, K., Niedrig, M., Swanepoel, R., 2007. Coronavirus antibodies in African bat species. Emerg. Infect. Dis. 13, 1367–1370.
Murakami, T., Ockinger, J., Yu, J., Byles, V., McColl, A., Hofer, A.M., Horng, T., 2012. Critical role for calcium mobilization in activation of the NLRP3 inflammasome. Proc. Natl. Acad. Sci. USA 109, 11282–11287.
Nal, B., Chan, C., Kien, F., Siu, L., Tse, J., Chu, K., Kam, J., Staropoli, I., Crescenzo-Chaigne, B., Escriou, N., van der Werf, S., Yuen, K.Y., Altmeyer, R., 2005. Differential maturation and subcellular localization of severe acute respiratory syndrome coronavirus surface proteins S, M and E. J. Gen. Virol. 86, 1423–1434.
Narayanan, K., Maeda, J., Maeda, A., Makino, S., 2000. Mechanism of specific coronavirus RNA packaging into virus particles. In: Proceedings of the 19th Annual Meeting American Society for Virology. Colorado, pp. 84.
Netland, J., DeDiego, M.L., Zhao, J., Fett, C., Alvarez, E., Nieto-Torres, J.L., Enjuanes, L., Perlman, S., 2010. Immunization with an attenuated severe acute respiratory syndrome coronavirus deleted in E protein protects against lethal respiratory disease. Virology 399, 120–128.
Nguyen, V.P., Hogue, B.G., 1997. Protein interactions during coronavirus assembly. J. Virol. 71, 9278–9284.
Nieto-Torres, J.L., DeDiego, M.L., Alvarez, E., Jimenez-Guardeño, J.M., Regla-Nava, J.A., Llorente, M., Kremer, L., Shuo, S., Enjuanes, L., 2011. Subcellular location and topology of severe acute respiratory syndrome coronavirus envelope protein. Virology 415, 69–82.
Nieto-Torres, J.L., Dediego, M.L., Verdia-Baguena, C., Jimenez-Guardeño, J.M., Regla-Nava, J.A., Fernandez-Delgado, R., Castaño-Rodriguez, C., Alcaraz, A., Torres, J., Aguilella, V.M., Enjuanes, L., 2014. Severe acute respiratory syndrome coronavirus envelope protein ion channel activity promotes virus fitness and pathogenesis. PLoS Pathog. 10, e1004077.
Nieva, J.L., Madan, V., Carrasco, L., 2012. Viroporins: structure and biological functions. Nat. Rev. Microbiol. 10, 563–574.
Paroutis, P., Touret, N., Grinstein, S., 2004. The pH of the secretory pathway: measurement, determinants, and regulation. Physiology (Bethesda) 19, 207–215.
Perlman, S., Netland, J., 2009. Coronaviruses post-SARS: update on replication and pathogenesis. Nat. Rev. Microbiol. 7, 439–450.

Pervushin, K., Tan, E., Parthasarathy, K., Lin, X., Jiang, F.L., Yu, D., Vararattanavech, A., Soong, T.W., Liu, D.X., Torres, J., 2009. Structure and inhibition of the SARS coronavirus envelope protein ion channel. PLoS Pathog. 5, e1000511.

Pugin, J., Ricou, B., Steinberg, K.P., Suter, P.M., Martin, T.R., 1996. Proinflammatory activity in bronchoalveolar lavage fluids from patients with ARDS, a prominent role for interleukin-1. Am. J. Respir. Crit. Care Med. 153, 1850–1856.

Quan, P.L., Firth, C., Street, C., Henriquez, J.A., Petrosov, A., Tashmukhamedova, A., Hutchison, S.K., Egholm, M., Osinubi, M.O., Niezgoda, M., Ogunkoya, A.B., Briese, T., Rupprecht, C.E., Lipkin, W.I., 2010. Identification of a severe acute respiratory syndrome coronavirus-like virus in a leaf-nosed Bat in Nigeria. mBio 1, e00208–e00210.

Queralt-Martin, M., Garcia-Gimenez, E., Mafe, S., Alcaraz, A., 2011. Divalent cations reduce the pH sensitivity of OmpF channel inducing the pK(a) shift of key acidic residues. Phys. Chem. Chem. Phys. 13, 563–569.

Raamsman, M.J.B., Locker, J.K., de Hooge, A., de Vries, A.A.F., Griffiths, G., Vennema, H., Rottier, P.J.M., Locker, J.K., de Hooge, A., de Vries, A.A.F., Griffiths, G., Vennema, H., Rottier, P.J.M., 2000. Characterization of the coronavirus mouse hepatitis virus strain A59 small membrane protein. E. J. Virol. 74, 2333–2342.

Regla-Nava, J.A., Nieto-Torres, J.L., Jimenez-Guardeño, J.M., Fernandez-Delgado, R., Fett, C., Castaño-Rodriguez, C., Perlman, S., Enjuanes, L., DeDiego, M.L., 2015. SARS coronaviruses with mutations in E protein are attenuated and promising vaccine candidates. J. Virol. 89, 3870–3887.

Rota, P.A., Oberste, M.S., Monroe, S.S., Nix, W.A., Campganoli, R., Icenogle, J.P., Peñaranda, S., Bankamp, B., Maher, K., Chen, M.-H., Tong, S., Tamin, A., Lowe, L., Frace, M., DeRisi, J.L., Chen, Q., Wang, D., Erdman, D.d., Peret, T.C.T., Burns, C., Ksiazek, T.G., Rollin, P.E., Sanchez, A., Liffick, S., Holloway, B., Limor, J., McCaustland, K., Olsen-Rassmussen, M., Fouchier, R., Gunther, S., Osterhaus, A.D.M.E., Drosten, C., Pallansch, M.A., Anderson, L.J., Bellini, W.J., 2003. Characterization of a novel coronavirus associated with severe acute respiratory syndrome. Science 300, 1394–1399.

Ruch, T.R., Machamer, C.E., 2012. The Coronavirus E protein: assembly and beyond. Viruses 4, 363–382.

Sakaguchi, T., Leser, G.P., Lamb, R.A., 1996. The ion channel activity of the influenza virus M2 protein affects transport through the Golgi apparatus. J. Cell Biol. 133, 733–747.

Schapiro, F.B., Grinstein, S., 2000. Determinants of the pH of the Golgi complex. J. Biol. Chem. 275, 21025–21032.

Scobey, T., Yount, B.L., Sims, A.C., Donaldson, E.F., Agnihothram, S.S., Menachery, V. D., Graham, R.L., Swanstrom, J., Bove, P.F., Kim, J.D., Grego, S., Randell, S.H., Baric, R.S., 2013. Reverse genetics with a full-length infectious cDNA of the Middle East respiratory syndrome coronavirus. Proc. Natl. Acad. Sci. USA 110, 16157–16162.

Strowig, T., Henao-Mejia, J., Elinav, E., Flavell, R., 2012. Inflammasomes in health and disease. Nature 481, 278–286.

Surya, W., Li, Y., Verdia-Baguena, C., Aguilella, V.M., Torres, J., 2015. MERS coronavirus envelope protein has a single transmembrane domain that forms pentameric ion channels. Virus Res. 201, 61–66.

Torres, J., Maheswari, U., Parthasarathy, K., Ng, L., Liu, D.X., Gong, X., 2007. Conductance and amantadine binding of a pore formed by a lysine-flanked transmembrane domain of SARS coronavirus envelope protein. Protein Sci. 16, 2065–2071.

Triantafilou, K., Kar, S., Vakakis, E., Kotecha, S., Triantafilou, M., 2013a. Human respiratory syncytial virus viroporin SH: a viral recognition pathway used by the host to signal inflammasome activation. Thorax 68, 66–75.

Triantafilou, K., Kar, S., van Kuppeveld, F.J., Triantafilou, M., 2013b. Rhinovirus-induced calcium flux triggers NLRP3 and NLRC5 activation in Bronchial cells. Am. J. Respir. Cell Mol. Biol. 49 (6) 923–934. 〈http://dx.doi.org/10.1165/rcmb.2013-0032OC〉.

Triantafilou, K., Triantafilou, M., 2014. Ion flux in the lung: virus-induced inflammasome activation. Trends Microbiol. 22, 580–588.

Venkatagopalan, P., Daskalova, S.M., Lopez, L.A., Dolezal, K.A., Hogue, B.G., 2015. Coronavirus envelope (E) protein remains at the site of assembly. Virology 478, 75–85.

Verdia-Baguena, C., Nieto-Torres, J.L., Alcaraz, A., Dediego, M.L., Enjuanes, L., Aguilella, V.M., 2013. Analysis of SARS-CoV E protein ion channel activity by tuning the protein and lipid charge. Biochim. Biophys. Acta 1828, 2026–2031.

Verdia-Baguena, C., Nieto-Torres, J.L., Alcaraz, A., Dediego, M.L., Torres, J., Aguilella, V.M., Enjuanes, L., 2012. Coronavirus E protein forms ion channels with functionally and structurally-involved membrane lipids. Virology 432, 485–494.

Wang, C., Lamb, R.A., Pinto, L.H., 1994. Direct measurement of the influenza A virus M2 protein ion channel activity in mammalian cells. Virology 205, 133–140.

Watanabe, S., Watanabe, T., Kawaoka, Y., 2009. Influenza A virus lacking M2 protein as a live attenuated vaccine. J. Virol. 83, 5947–5950.

Whitehead, S.S., Bukreyev, A., Teng, M.N., Firestone St, C.Y., Claire, M., Elkins, W.R., Collins, P.L., Murphy, B.R., 1999. Recombinant respiratory syncytial virus bearing a deletion of either the NS2 or SH gene is attenuated in chimpanzees. J. Virol. 73, 3438–3442.

Wilson, L., Gage, P., Ewart, G., 2006. Hexamethylene amiloride blocks E protein ion channels and inhibits coronavirus replication. Virology 353, 294–306.

Wilson, L., McKinlay, C., Gage, P., 2004. SARS coronavirus E protein forms cation-selective ion channels. Virology 330, 322–331.

Wong, S.K., Li, W., Moore, M.J., Choe, H., Farzan, M., 2004. A 193-amino acid fragment of the SARS coronavirus S protein efficiently binds angiotensin-converting enzyme 2. J. Biol. Chem. 279, 3197–3201.

Wozniak, A.L., Griffin, S., Rowlands, D., Harris, M., Yi, M., Lemon, S.M., Weinman, S. A., 2010. Intracellular proton conductance of the hepatitis C virus p7 protein and its contribution to infectious virus production. PLoS Pathog. 6, e1001087.

Wu, Y.H., Kuo, W.C., Wu, Y.J., Yang, K.T., Chen, S.T., Jiang, S.T., Gordy, C., He, Y.W., Lai, M.Z., 2014. Participation of c-FLIP in NLRP3 and AIM2 inflammasome activation. Cell Death Differ. 21, 451–461.

Wuytack, F., Raeymaekers, L., Missiaen, L., 2002. Molecular physiology of the SERCA and SPCA pumps. Cell Calcium 32, 279–305.

Yount, B., Roberts, R.S., Sims, A.C., Deming, D., Frieman, M.B., Sparks, J., Denison, M. R., Davis, N., Baric, R.S., 2005. Severe acute respiratory syndrome coronavirus group-specific open reading frames encode nonessential functions for replication in cell cultures and mice. J. Virol. 79, 14909–14922.

Zaki, A.M., van Boheemen, S., Bestebroer, T.M., Osterhaus, A.D., Fouchier, R.A., 2012. Isolation of a novel coronavirus from a man with pneumonia in Saudi Arabia. N. Engl. J. Med. 367, 1814–1820.

Zhou, Y., Frey, T.K., Yang, J.J., 2009. Viral calciomics: interplays between Ca^{2+} and virus. Cell Calcium 46, 1–17.